

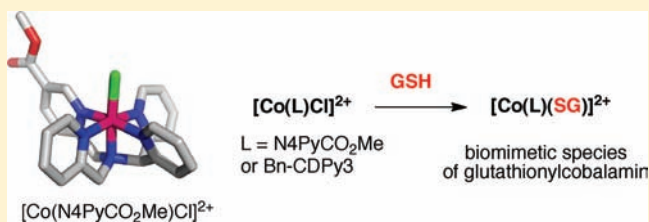
Synthesis, Characterization, and Glutathionylation of Cobalamin Model Complexes $[\text{Co}(\text{N4PyCO}_2\text{Me})\text{Cl}]\text{Cl}_2$ and $[\text{Co}(\text{Bn-CDPy3})\text{Cl}]\text{Cl}_2$

Jai Prakash and Jeremy J. Kodanko*

Department of Chemistry, Wayne State University, 5101 Cass Avenue, Detroit, Michigan 48202, United States

Supporting Information

ABSTRACT: Synthetic Co(III) complexes containing N5 donor sets undergo glutathionylation to generate biomimetic species of glutathionylcobalamin (GSCbl), an important form of cobalamin (Cbl) found in nature. For this study, a new Co(III) complex was synthesized derived from the polypyridyl pentadentate N5 ligand N4PyCO₂Me (1). The compound $[\text{Co}(\text{N4PyCO}_2\text{Me})\text{Cl}]\text{Cl}_2$ (3) was characterized by X-ray crystallography, UV-vis, IR, ¹H NMR, and ¹³C NMR spectroscopies and mass spectrometry (HRMS). Reaction of 3 with glutathione (GSH) in H₂O generates the biomimetic species $[\text{Co}(\text{N4PyCO}_2\text{Me})(\text{SG})]^{2+}$ (5), which was generated *in situ* and characterized by UV-vis and ¹H NMR spectroscopies and HRMS. ¹H NMR and UV-vis spectroscopic data are consistent with ligation of the cysteine thiolate of GSH to the Co(III) center of 5, as occurs in GSCbl. Kinetic analysis indicated that the substitution of chloride by GS⁻ occurs by a second-order process [$k_1 = (10.1 \pm 0.7) \times 10^{-2} \text{ M}^{-1} \text{ s}^{-1}$]. The observed equilibrium constant for formation of 5 ($K_{\text{obs}} = 870 \pm 50 \text{ M}^{-1}$) is about 3 orders of magnitude smaller than for GSCbl. Reaction of the Co(III) complex $[\text{Co}(\text{Bn-CDPy3})\text{Cl}]\text{Cl}_2$ (4) with GSH generates glutathionylated species $[\text{Co}(\text{Bn-CDPy3})(\text{GS})]^{2+}$ (6), analogous to 5. Glutathionylation of 4 occurs at a similar rate [$k_2 = (8.4 \pm 0.5) \times 10^{-2} \text{ M}^{-1} \text{ s}^{-1}$], and the observed equilibrium constant ($K_{\text{obs}} = 740 \pm 47 \text{ M}^{-1}$) is slightly smaller than for 5. Glutathionylation showed a significant pH dependence, where rates increased with pH. Taken together, these results suggest that glutathionylation is a general reaction for Co(III) complexes related to Cbl.



INTRODUCTION

Vitamin B₁₂ is a key cofactor in humans, deficiency of which may lead to destruction of parietal cells in the stomach (pernicious anemia) and neurological disorders such as Alzheimer's disease.^{1–3} Recently, vitamin B₁₂ deficiency was also associated with an increased risk of prostate cancer.⁴ Vitamin B₁₂ serves as a coenzyme for two major enzymatic reactions in mammals: methylcobalamin (MeCbl) mediated transfer of a methyl group from methyltetrafolate to homocysteine by methionine synthase to generate methionine, and adenosylcobalamin (AdoCbl) mediated isomerization of methylmalonyl CoA to succinyl CoA, which is catalyzed by methylmalonyl CoA synthase.^{5–8} High serum levels of homocysteine that result from vitamin B₁₂ deficiency are associated with an increased risk of myocardial infarction and cerebral strokes.^{9–11} Homocysteine also inhibits the enzymes superoxide dismutase and glutathione peroxidase, known for their antioxidant activity, promoting the formation of reactive oxygen species and activating endothelial proinflammatory signaling pathways.^{12,13} Patients suffering from Alzheimer's disease have been found to have moderately high levels of homocysteine.^{14–17}

Because mammals cannot synthesize Cbl, and Cbl is too polar to pass through the cell plasma membrane, a complex pathway for gastrointestinal absorption, blood transport, and cellular uptake of dietary Cbl evolved.¹⁸ Cell surface receptors and Cbl-transport proteins act in a cascade to shuttle Cbl from

the gut, through the bloodstream and into specific locations in cells.^{19–21} During the processes of transport, uptake, and biological utilization, Cbl is known to take many forms. Cbls each have an N5 donor atoms set composed of one benzimidazole and four corrin ring nitrogen atoms, and vary according to the sixth donor group (X, Figure 1) bound to the cobalt center. Known derivatives include MeCbl (X = Me), AdoCbl (X = 5'-deoxyadenosine), aquacobalamin (X = H₂O), and cyanocobalamin (X = CN), also known as vitamin B₁₂. Another important example is thiolate-ligated species glutathionylcobalamin (GSCbl), which forms rapidly upon reaction of glutathione (GSH) with aquacobalamin (H₂OcbI⁺). Due to the fact that GSH is abundant in cells, reaching concentrations as high as 10 mM,^{22,23} GSCbl is thought to be an important form of cobalamin present in cells that is not protected by a transport protein or within an organelle. Indeed, GSCbl was recently isolated from cultured endothelial cells²⁴ and shown to elicit potent antioxidant properties *in vitro*.²⁵ GSCbl has also been proposed as an intermediate in the biosynthesis of active cobalamin coenzymes, AdoCbl and MeCbl,²⁶ where it was suggested that GSCbl is a more direct precursor of the coenzyme promoting methyl synthase activity. Hence, GSCbl might be more effective than other cobalamins in treatment of

Received: December 12, 2011

Published: February 8, 2012

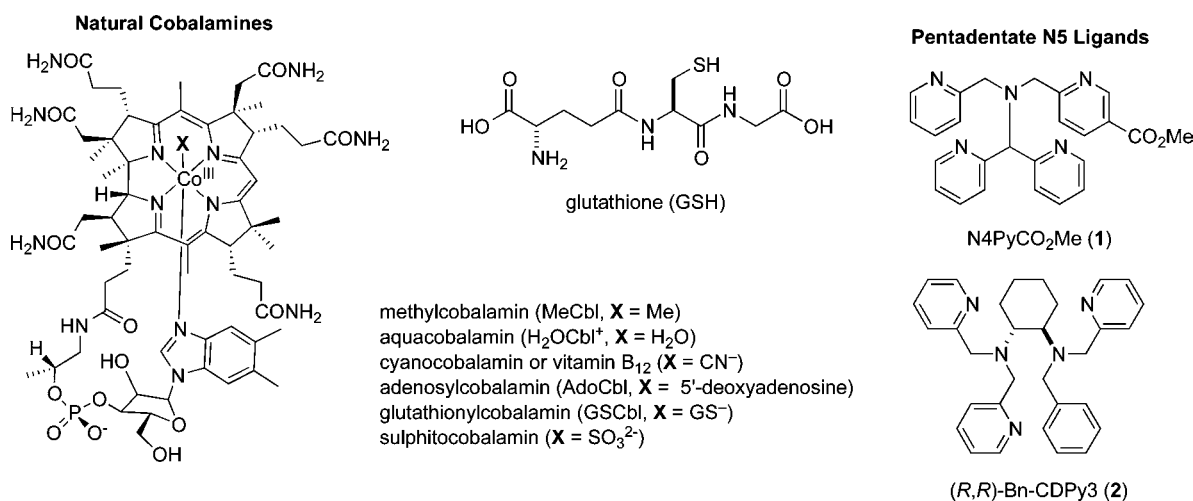


Figure 1. Structure of the cobalamines, glutathione (GSH), and pentadentate N5 donor ligands N4PyCO₂Me (1) and (R,R)-Bn-CDPy3 (2).

conditions associated with hyperhomocysteinemia and oxidative stress, including dementia, arthritis, and cancer.^{3,27}

Structural and chemical properties of GSCbl have been investigated by a number of laboratories. Unlike other thiolatocobalamines, GSCbl has been found to be unusually stable at pH 7.2 at 25 °C (i.e., $t_{1/2}\text{GSCbl}/t_{1/2}\text{CysCbl} > 6 \times 10^4$), most probably due to the favorable interactions of their terminal carboxylates with the corrin side chains.^{28–31} However, GSCbl, like other thiolatocobalamines, decomposes spontaneously to H₂OCbl⁺ at pH < 3 and is unlikely to sustain the acidic environment found in the stomach (pH < 2).^{32,33} GSCbl can be synthesized by treating H₂OCbl⁺ with GSH.^{26,31,34–36} Thermodynamic and kinetic parameters of GSCbl formation from H₂OCbl⁺ and GSH have been measured.^{31,37,38} A large formation constant ($K_f = 5 \times 10^9 \text{ M}^{-1}$) and bimolecular rate constants as high as $163 \pm 8 \text{ M}^{-1} \text{ s}^{-1}$ have been reported recently, concluding that GSCbl formation from H₂OCbl⁺ is both rapid and highly favorable.³⁷ The nature of this reaction suggests that any free intracellular H₂OCbl⁺ (H₂OCbl⁺ not attached to protein) is prone to conversion to GSCbl, as GSH is found up to 10 mM in concentration in most biological tissues. However, the extent of this facile conversion may be limited in cells by the fact that free Cbl is estimated to be <5%.³⁸ GSCbl also reacts with NO with second-order rate constant of $2.82 \times 10^3 \text{ M}^{-1} \text{ s}^{-1}$ and has the ability to reverse the biological effect caused by NO.³⁹ The structure of GSCbl was supported by thorough spectroscopic studies^{29,36,40} and density functional theory (DFT) calculations,^{41,42} and later confirmed by X-ray crystallographic analysis,⁴³ to include thiolate binding of the cysteine residue present in GSH to the Co(III) center of Cbl. In addition, electronic absorption, circular dichroism, magnetic circular dichroism, and resonance Raman spectroscopic data were obtained recently for GSCbl.⁴⁴ These data were correlated with DFT calculations to complete a description of the electronic structure of GSCbl.

A number of cobalt(III) complexes have been synthesized as models for vitamin B₁₂.^{45–65} Ligand substitution reactions with various nucleophiles (SCN⁻, N₃⁻, OH⁻, CN⁻, pyridine, 2-aminopyridine, diethoxyethylamine, NH₃, 2-mercaptoethanol, etc.) have been studied to understand the reactivity at the Co(III) center of the vitamin B₁₂ coenzyme. Kinetic and equilibrium studies for axial thiolate ligation of methylaquacobaloxime were reported, where the thiols used for ligation were

2-mercaptoethanol, S-methyl-2-mercaptoethanol, mercaptoacetate, and methylmercaptoacetate.⁴⁷ Although the interaction of glutathione with a vitamin B₁₂ model complex has been documented,⁶⁶ a detailed kinetic and thermodynamic study on glutathionylation with synthetic vitamin B₁₂ model complexes has never been reported. In this Article, we report the interesting observation that glutathionylation is not unique to Cbl, but in fact occurs readily with a series of other Co(III) complexes that mimic the structure of this important biological cofactor. In this study, the synthesis and characterization of a new Co(III) complex is described, which is derived from the polypyridyl pentadentate N5 ligand N4PyCO₂Me (1) (Figure 1). The complex [Co(N4PyCO₂Me)Cl]Cl₂ (3) and related congener [Co(Bn-CDPy3)Cl]Cl₂ (4), which contain an N5 coordination environment like that of Cbl, undergo biomimetic reactions with GSH to generate the species [Co(N4PyCO₂Me)(SG)]²⁺ (5) and [Co(Bn-CDPy3)(SG)]²⁺ (6), respectively. Species 5 and 6 were generated *in situ* and characterized in solution. Data for 5 and 6 are consistent with the cysteine thiolate in GSH binding to the Co(III) centers of these complexes. Kinetic and thermodynamic studies for glutathionylation of 3 and 4 are reported, and relevance of these data to the analogous reaction with H₂OCbl⁺ is discussed. To the best of our knowledge, this is the first example of synthetic Co(III) coordination complexes based on polypyridyl ligands mimicking the behavior of Cbl and undergoing glutathionylation with GSH.

EXPERIMENTAL SECTION

General Considerations. All reagents were purchased from commercial suppliers and used as received. Ligands N4PyCO₂Me (1)⁶⁷ and (R,R)-Bn-CDPy3 (2)⁶⁸ and the complex [Co(Bn-CDPy3)Cl]Cl₂ (4)^{68,69} were prepared using literature procedures. NMR spectra were recorded on a Varian FT-NMR Mercury-400 MHz spectrometer. Mass spectra were recorded on a Waters ZQ2000 single quadrupole mass spectrometer using an electrospray ionization source. IR spectra were recorded on a Nicolet FT-IR spectrophotometer. All reactions were performed under ambient atmosphere unless otherwise noted. Conductivity measurements were performed with an Omega portable conductivity meter (model CDH-280). X-ray diffraction data were collected on a Bruker APEX-II diffractometer at 100 K. Kinetic and thermodynamic studies have been performed in 100 mM acetate buffer (pH 5.0, I = 100 mM (KNO₃)) unless otherwise noted.

Synthesis of [Co(N4PyCO₂Me)Cl]Cl₂ (3). The compound, *trans*-[Co(Py)₄Cl₂]Cl·6H₂O,^{70,71} (277 mg, 0.47 mmol) was added to a

solution of **1** (200 mg, 0.47 mmol) in CH_2Cl_2 (5 mL). The mixture was stirred for 60 min, during which time a light purple solid formed. The resultant solid was isolated by filtration in analytically pure form (173 mg, 71%). Single crystals of **3** suitable for X-ray crystallographic analysis were obtained by recrystallization of the purple precipitate from EtOH with Et₂O vapor diffusion, followed by isolation of the pink solid and recrystallization from MeOH with Et₂O vapor diffusion. Mp = 144–146 °C. ¹H NMR (CD_3OD) δ 9.94 (s, 1H), 9.47 (d, J = 5.67 Hz, 1H), 8.90 (t, J = 8.92 Hz, 2H), 8.49 (dd, J = 6.48, 1.62 Hz, 1H), 8.25–8.34 (m, 4H), 7.99 (dt, J = 1.62, 7.19 Hz, 1H), 7.69 (t, J = 6.48, 1H), 7.6–7.66 (m, 3H), 7.46 (d, J = 8.1 Hz, 1H), 7.07 (s, 1H), 5.13–5.43 (m, 4H), 4.01 (s, 3H). ¹³C NMR (CD_3OD) δ 169.9, 166.4, 160.8, 160.7, 156.5, 156.4, 153.4, 152.8, 144.2, 142.5, 142.4, 130.9, 128.7, 128.5, 127.0, 125.1, 81.1, 67.6, 67.5, 53.7 ppm. IR (KBr) 3588 (w), 3568 (w), 3407 (s), 2922 (m), 1735 (s), 1610 (s), 1300 (s) cm^{-1} . HRMS (ESMS) calcd for $\text{C}_{25}\text{H}_{23}\text{O}_2\text{N}_5\text{CoCl}$ (M^{2+}) 259.5436, found 259.5437. Anal. Calcd for $\text{C}_{25}\text{H}_{28}\text{Cl}_3\text{CoN}_5\text{O}_{4.5}$ ($2 \cdot 2.5\text{H}_2\text{O}$): C, 47.23; H, 4.44; N, 11.01. Found: C, 47.21; H, 4.19; N, 10.95.

Kinetic Studies. Generation of the complexes $[\text{Co}(\text{N4PyCO}_2\text{Me})(\text{SG})]^{2+}$ (**5**) and $[\text{Co}(\text{Bn-CDPy3})(\text{SG})]^{2+}$ (**6**), formed *in situ* from reaction of GSH with **3** and **4**, respectively, were followed spectrophotometrically. The solutions of **3** or **4** (1 mM, 50 μL , final concentrations = 0.5 mM) in 100 mM acetate buffer were treated with solutions of GSH in the same buffer (50 μL , final concentration = 0–25 mM). Absorbance at 323 nm for formation of **5** and 320 nm for formation of **6** was recorded over a period of 2 h at 298 ± 2 K with a GENios Pro microplate reader (TECAN) using a 96 well microplate. All data were collected in triplicate. Initial rates of reaction were calculated from slopes obtained from linear portions of absorbance ($A_{320/323}$) versus time graphs for the first 5% of the reaction (see Supporting Information for detailed calculation).

Determination of Equilibrium Constant (K_{obs}). The observed equilibrium constants for the formation of glutathionylated products **5** and **6** were determined by measuring the absorbances of equilibrated reaction mixtures containing cobalt complexes **3** or **4** (0.5 mM) and GSH (0–15 mM or 25 mM, respectively) in 100 mM acetate buffer. $A_{323/320}$ values were plotted against $[\text{GSH}]$, and the data were fit according to literature methods.³⁷

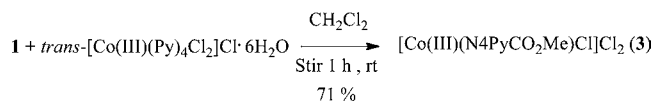
¹H NMR Spectroscopic Studies. A solution of GSH (12.3 mg, 40 μmol) and **3** (5.9 mg, 10 μmol) or **4** (6.4 mg, 10 μmol) in D_2O (1 mL) was prepared. The reaction was monitored by ¹H NMR spectroscopy at regular time intervals. The reaction was maintained at room temperature (298 ± 2 K) during the experiment.

X-ray Crystallographic Studies. Diffraction data were collected on a Bruker X8 APEX-II kappa geometry diffractometer equipped with Mo radiation and a graphite monochromator at 100 K. Frames were recorded for 10 s and 0.3° between frames. APEX-II and SHELX software^{72,73} were used in the collection and refinement of the model. Crystals of **3** appeared as red rhomboids. Reflections (36 734) were measured, of which 7571 were independent. Hydrogen atoms were placed in calculated positions. The asymmetric unit contains one coordination complex, two Cl anions, and one equivalent each of methanol and ethanol. The ethanol was disordered over two sites and described with partial occupancies and isotropic thermal parameters. There is a network of hydrogen bonds linking the anions and solvates in the lattice.

RESULTS

Synthesis of **3.** The Co(III) complex, $[\text{Co}(\text{III})(\text{N4PyCO}_2\text{Me})\text{Cl}]_2$ (**3**), where N4PyCO₂Me (**1**) is methyl 6-(((di(pyridin-2-yl)methyl)(pyridin-2-ylmethyl)amino)-methyl)nicotinate, was synthesized using the Co(III) starting material *trans*- $[\text{Co}(\text{Py})_4\text{Cl}_2]\text{Cl} \cdot 6\text{H}_2\text{O}$, (Scheme 1). Stirring the ligand **1** with 1 equiv of *trans*- $[\text{Co}(\text{Py})_4\text{Cl}_2]\text{Cl} \cdot 6\text{H}_2\text{O}$ in CH_2Cl_2 for 60 min at room temperature resulted in the formation of **3** as a pink precipitate. Recrystallization of this pink solid by vapor diffusion of Et₂O into EtOH, followed by Et₂O into

Scheme 1. Synthesis of $[\text{Co}(\text{III})(\text{N4PyCO}_2\text{Me})\text{Cl}]_2$ (**3**)



MeOH, gave pink crystals of **3** suitable for X-ray crystallographic analysis.

UV–Vis Spectroscopic Data. The compound **3**, typical of other low spin Co(III) complexes, shows two major absorption bands, λ_{max} at 370 and 520 nm with extinction coefficient, ϵ , 340 $\text{M}^{-1} \text{cm}^{-1}$ and 210 $\text{M}^{-1} \text{cm}^{-1}$, respectively (Figure 2) in

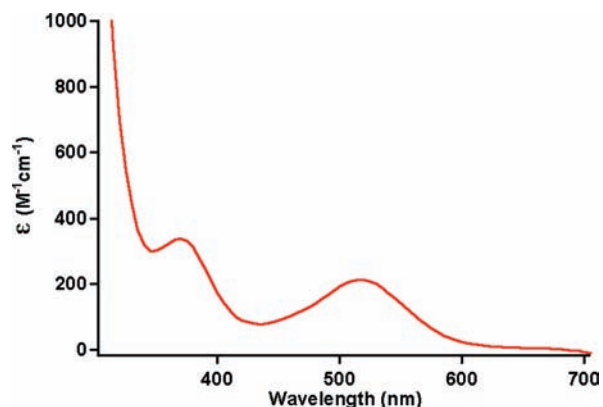


Figure 2. UV–vis spectrum of **3** in MeOH (1 mM) at 298 ± 2 K.

MeOH. These bands are assigned to transitions from the $^1\text{A}_{1g}$ ground state to the upper $^1\text{T}_{1g}$ and $^1\text{T}_{2g}$ states in the parent octahedral species, on the basis of analogy with related Co(III) complexes.^{74,75}

¹H NMR and ¹³C NMR Spectroscopic Data. The ¹H NMR spectrum of **3** in CD_3OD revealed that resonances were sharp and well resolved and lie between 3.9 and 9.9 ppm, consistent with a diamagnetic low spin Co(III) complex. Likewise, resonances observed in the ¹³C NMR spectrum of **3** lie between 54 and 170 ppm. The most important features of these resonances, both in ¹H NMR (Figure 3) and ¹³C NMR

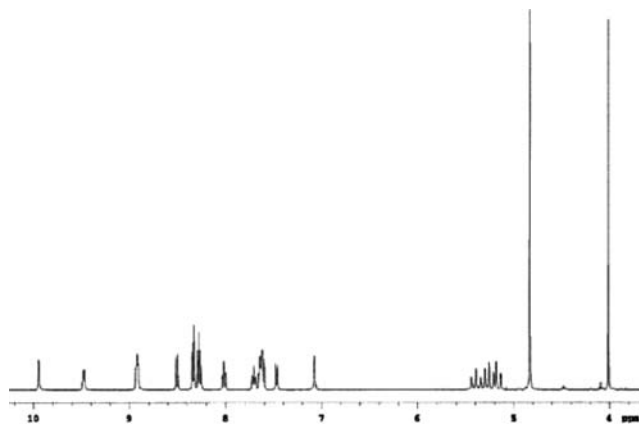


Figure 3. ¹H NMR spectrum of **3** in CD_3OD .

spectra (SI), are that they are shifted downfield in **3** when compared with the parent ligand **1**, consistent with the pyridine N-atoms remaining bound to the metal center in solution. Resonances assigned to the H-atoms located at the 2-position of the four pyridine rings shift by approximately 1 ppm when

compared with the spectrum of **1**, consistent with the hypothesis that all four pyridine rings remain bound to the Co(III) center. Particularly striking is the 1.71 ppm downfield shift of the methine C–H resonance, from 5.36 ppm in the parent ligand **1** to 7.07 ppm in complex **3**. In addition, the four methylene protons of the ligand become diastereotopic upon coordination to the metal center, and each proton shows a unique resonance in complex **3** (5.13–5.43 ppm). Typical coupling values of 16–19 Hz for geminal protons are observed, consistent with the chiral properties of **3**, which unlike symmetric complexes of N4Py, does not possess a mirror plane due to the ester substituent.

HRMS Data. The high-resolution electrospray ionization mass spectrum (ESI-MS) for **3** in H₂O solution reveals a prominent ion cluster with a dominant peak at *m/z* 259.5437. This cluster displayed an isotopic pattern that fits with molecular formula [Co(N4PyCO₂Me)Cl]²⁺ (Figure 4). It is noteworthy that the axially coordinated Cl[−] ligand remains attached in solution.

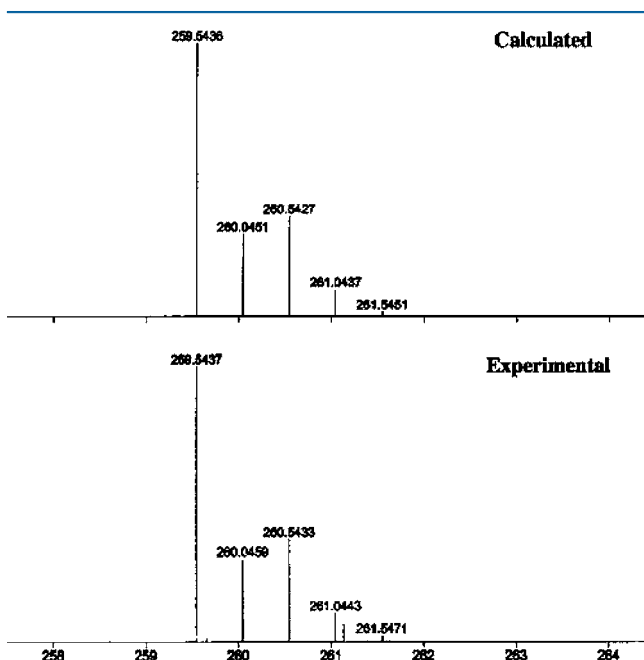


Figure 4. Calculated (top) and observed (bottom) high resolution mass spectra (HRMS) for the dication [Co(N4PyCO₂Me)Cl]²⁺ of **3**.

X-ray Crystallographic Data. Crystallographic data for **3** are given in Table 1. Tables 2 and 3 list selected bond lengths and bond angles, respectively. Complex **3** crystallized in the space group *P* $\bar{1}$, with *Z* = 2. Figure 5 shows an ORTEP diagram of the dication [Co(N4PyCO₂Me)Cl]²⁺.

The Co(III) center of the dication [Co(N4PyCO₂Me)Cl]²⁺ has an N5Cl donor atom set. Bond lengths are consistent with a low-spin Co(III) ion. The octahedral geometry is slightly distorted, due to acute bite angles typical of 5-membered rings. The angles between Cl(1) and N(4–5) are approximately 3° smaller than angles involving N(2–3), resulting from the restriction of the common atom C(15). Even though the environments are dissimilar, bond lengths between Co(1) and all the five nitrogen donors of N4PyCO₂Me are nearly identical, varying from 1.930(2) to 1.938(2) Å, indicating that the ester moiety on the pyridine ring of the ligand does not affect the bond length between Co(1) and N(2) to a great extent. These

Table 1. Crystal Data and Structure Refinement for **3**·MeOH·EtOH

empirical formula	C ₂₈ H ₃₃ Cl ₃ CoN ₅ O ₄
fw	668.87
cryst syst	triclinic
space group	<i>P</i> $\bar{1}$
<i>a</i> (Å)	9.6350(3)
<i>b</i> (Å)	11.5595(4)
<i>c</i> (Å)	15.6403(5)
α (deg)	97.695(2)
β (deg)	106.955(1)
γ (deg)	109.816(2)
<i>V</i> (Å ³)	1514.23(9)
<i>Z</i>	2
<i>D</i> _{calc} (mg/m ³)	1.467
abs coeff, μ (mm ^{−1})	0.874
<i>F</i> (000)	692
cryst size (mm ³)	0.29 × 0.26 × 0.18
θ -range for data collection (deg)	1.94–28.48
limiting indices	−12 ≤ <i>h</i> ≤ 12, −15 ≤ <i>k</i> ≤ 15, 0 ≤ <i>l</i> ≤ 20
unique reflns	36734/7571 [<i>R</i> (int) = 0.0342]
GOF on <i>F</i> _o ²	1.033
final <i>R</i> indices [<i>I</i> > 2 σ (<i>I</i>)]	<i>R</i> 1 = 0.0450, <i>wR</i> 2 = 0.1227
<i>R</i> indices (all data)	<i>R</i> 1 = 0.0530, <i>wR</i> 2 = 0.1269
highest peak and deepest hole (e Å ^{−3})	1.642 and −0.388

Table 2. Selected Bond Lengths (Å) of **3**

Co(1)–N(3)	1.930(2)
Co(1)–N(1)	1.933(2)
Co(1)–N(5)	1.933(2)
Co(1)–N(4)	1.933(2)
Co(1)–N(2)	1.938(2)
Co(1)–Cl(1)	2.222(6)

Table 3. Selected Bond Angles (deg) of **3**

N(3)–Co(1)–N(1)	86.40(8)	N(3)–Co(1)–N(5)	89.50(8)
N(1)–Co(1)–N(5)	83.55(9)	N(3)–Co(1)–N(4)	169.66(9)
N(3)–Co(1)–N(2)	91.52(8)	N(1)–Co(1)–N(2)	86.35(8)
N(5)–Co(1)–N(2)	169.76(9)	N(4)–Co(1)–N(2)	89.35(8)
N(3)–Co(1)–Cl(1)	96.33(6)	N(1)–Co(1)–Cl(1)	175.84(6)
N(5)–Co(1)–Cl(1)	93.32(6)	N(4)–Co(1)–Cl(1)	93.81(6)
N(2)–Co(1)–Cl(1)	96.70(6)	C(1)–N(1)–Co(1)	110.1(1)
C(9)–N(1)–Co(1)	110.0(1)	C(15)–N(1)–Co(1)	98.9(1)
C(2)–N(2)–Co(1)	112.9(2)	C(6)–N(2)–Co(1)	127.7(2)
C(14)–N(3)–Co(1)	127.1(2)	C(10)–N(3)–Co(1)	113.6(2)
C(20)–N(4)–Co(1)	128.6(2)	C(16)–N(4)–Co(1)	111.3(2)
C(25)–N(5)–Co(1)	128.9(2)	C(21)–N(5)–Co(1)	111.0(2)

Co–N lengths are decidedly short.⁷⁶ Furthermore, the Co–Cl bond length (2.222 Å) is at the very shortest end of the recorded ranges for similar complexes, which may indicate a strong Co–Cl bond.^{68,76–78} The Co ion lies 0.171(1) Å out of the N4 equatorial plane toward the Cl atom (cf., Ru displacement of 0.263 Å in RuN4PyCl).⁷⁹

Molar Conductivity Data. Molar conductivity (Λ _M) values for **3** in H₂O range from 133 to 180 S cm² mol^{−1} for concentrations ranging from 2.0 to 0.5 mM. These data agree well with the data for other 2:1 electrolytes in H₂O.⁸⁰ Importantly, these data are consistent with the dication of **3** maintaining its structure in solution, and not undergoing rapid

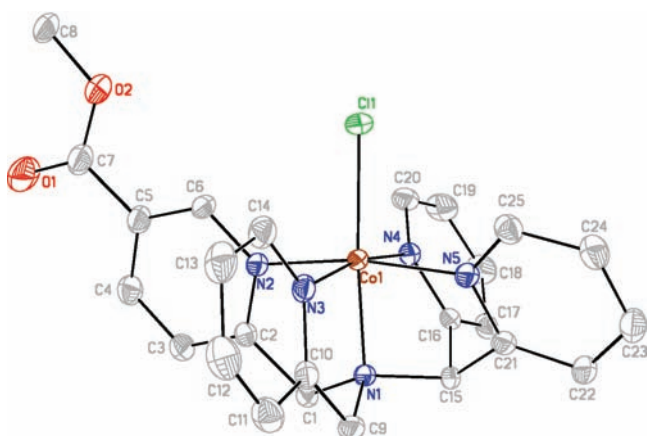
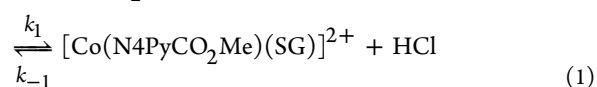
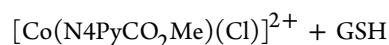


Figure 5. ORTEP diagram of the dication $[\text{Co}(\text{N4PyCO}_2\text{Me})\text{Cl}]^{2+}$, thermal ellipsoids are drawn at the 50% probability. Hydrogen atoms and chloride counterions have been omitted for clarity.

hydrolysis to form $[\text{Co}(\text{N4PyCO}_2\text{Me})(\text{H}_2\text{O})]^{3+}$, which would act as a 3:1 electrolyte.

Glutathionylation of Cobalt Complex 3. Treatment of the Co(III) complex **3** with GSH in 100 mM acetate buffer resulted in a color change from pink to brown within minutes at room temperature. Upon following the reaction of **3** (0.5 mM) with GSH (10 mM) by UV-vis spectroscopy, the disappearance of a peak at 520 nm and appearance of two new peaks at 323 and 440 nm with a shoulder at 490 nm were observed, with two isosbestic points at 490 and 560 nm (Figure 6a). These results are consistent with conversion of **3** into a new product without the formation of any long-lived intermediate. When the initial rates of the reaction of **3** (0.5 mM) with GSH (0.5–25 mM) were plotted against the total concentration of GSH, a line passing through the origin can be

fit, indicating the reaction (eq 1) to be first-order with respect to GSH. A second-order rate constant, k_1 , of $9.3 \times 10^{-2} \text{ M}^{-1} \text{ s}^{-1}$ was obtained from these data (Figure 6b, see SI for detailed calculation). Similarly, when the initial rates of reaction of GSH (4 mM) with **3** (0.5–4 mM) were plotted against concentration of **3**, a line passing through the origin can be fit, indicating the reaction to be first-order also with respect to **3**, and from these data, a second-order rate constant, k_1 , of $10.8 \times 10^{-2} \text{ M}^{-1} \text{ s}^{-1}$ was obtained (Figure 6c). The values of k_1 obtained from both the plots were in good agreement within the experimental error confirming that the reaction follows the rate law, $\text{rate} = k_1[\mathbf{3}][\text{GSH}]$ under the condition used in this study. It is noteworthy that this reaction is approximately 2 orders of magnitude slower than the reaction of GSH with H_2OCbl^+ .³⁷ Next, the observed equilibrium constant was determined for the reaction of **3** with GSH (eq 2) in 100 mM acetate buffer (Figure 6d). The value calculated for K_{obs} was $870 \pm 50 \text{ M}^{-1}$, which is approximately 3 orders of magnitude smaller than that of GSCbl ($9.5 \times 10^5 \text{ M}^{-1}$).³⁷



$$K_{\text{obs}}(\text{s}) = [\mathbf{5}]/([\mathbf{3}][\text{GSH}]) \quad (2)$$

Further examination revealed that rates for glutathionylation of **3** showed a significant dependence on pH. Studies carried out in the pH range 4.0–8.0 confirmed that the rates for the substitution reaction increased with increase in pH (SI). This was expected, because the concentration of the more nucleophilic thiolate GS^- ($\text{p}K_{\text{a}}$ of thiol of GSH = 8.72)⁸¹ increases with respect to the neutral thiol GSH at higher pH. It is important to note that conditions of these experiments are

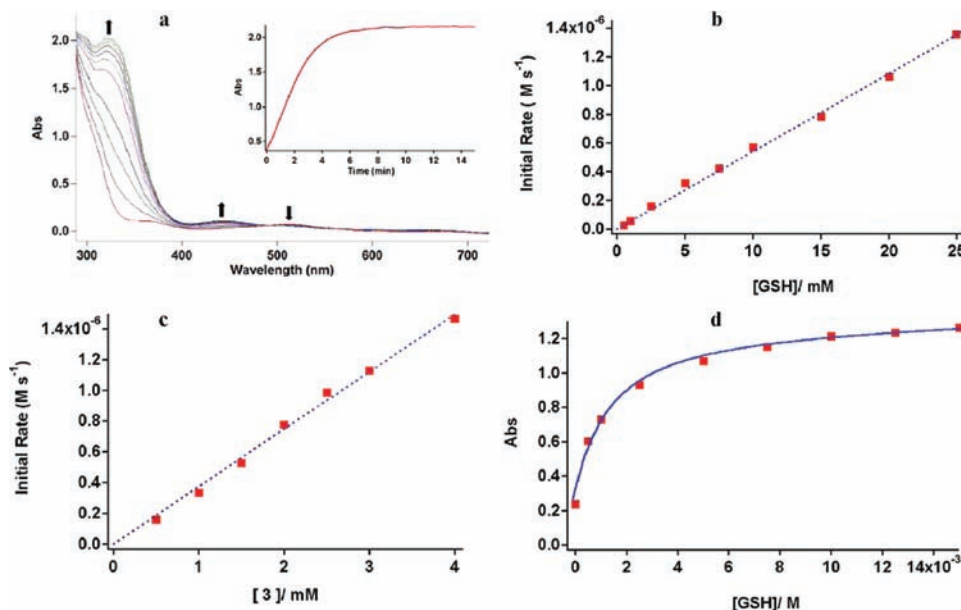


Figure 6. (a) UV-vis spectral change for **3** (0.5 mM) on reaction with GSH (10 mM) in 100 mM acetate buffer at $298 \pm 2 \text{ K}$ (inset: Abs vs time plot for growth of peak at 323 nm). (b) Plot of the initial rate of reaction vs $[\text{GSH}]$ for substitution of Cl^- with GSH (0.5–25 mM) in **3** (0.5 mM) in 100 mM acetate buffer to form $[\text{Co}(\text{N4PyCO}_2\text{Me})(\text{SG})]^{2+}$. (c) Plot of the initial rate of reaction vs $[\mathbf{3}]$ for substitution of Cl^- with GSH (4.0 mM) in **3** (0.5–4 mM) in 100 mM acetate buffer. (d) Abs_{323} vs $[\text{GSH}]$ plot, obtained from the equilibrated solutions of **3** (0.5 mM) and GSH (0.0–15 mM) kept at $298 \pm 2 \text{ K}$ for 2 h (the data were fit according to the literature method, fixing $[\mathbf{3}] = 5.0 \times 10^{-4} \text{ M}$, $A_{323}(\mathbf{3}) = 0.237$ and $A_{323}(\mathbf{5}) = 1.263$).³⁷

relevant to biology, because GSH is estimated to be present at concentrations much higher (up to 10^6) than H_2OCbl^+ in cells.

The species $[\text{Co}(\text{N4PyCO}_2\text{Me})(\text{SG})]^{2+}$ (**5**), obtained from reaction of **3** and GSH, was generated *in situ* and characterized further by UV-vis and ^1H NMR spectroscopies and mass spectrometry. The *in situ* generated **5**, obtained from the reaction of **3** with GSH, shows two major absorption bands, one intense at 323 nm and other relatively weaker at 440 nm with shoulder at 490 nm (Figure 6a). The intense peak at 323 nm is consistent with thiolate ligation to Co(III) in **5** and is assigned to $\text{S} \rightarrow \text{Co(III)}$ ligand-to-metal charge transfer (LMCT) transition based on analogy with other Co(III) complexes.^{47,66,82} The thiolate ligation in **5** was further corroborated by the fact that other thiols, i.e., *N*-acetylcysteine and 2-mercaptoethanol upon reaction with **3**, gave similar absorption bands. The weaker band at 440 nm with shoulder at 490 nm can be due to a splitting of the $^1\text{A}_{1g} \rightarrow ^1\text{T}_{1g}$ transition arising by a lowering of the symmetry from O_h , on the basis of literature assignments.^{82,83} Using the maximum absorbance observed for reaction of **3** (0.5 mM) with GSH (10 mM), a molar extinction coefficient of $\epsilon_{323} = 4300 \text{ M}^{-1} \text{ cm}^{-1}$, $\epsilon_{440} = 280 \text{ M}^{-1} \text{ cm}^{-1}$, and $\epsilon_{490} = 120 \text{ M}^{-1} \text{ cm}^{-1}$ was calculated for **5**, respectively.

^1H NMR spectra were recorded at regular time intervals to follow the reaction of **3** (10 mM) with GSH (40 mM) in D_2O (Figure 7). At the beginning of the reaction, no immediate

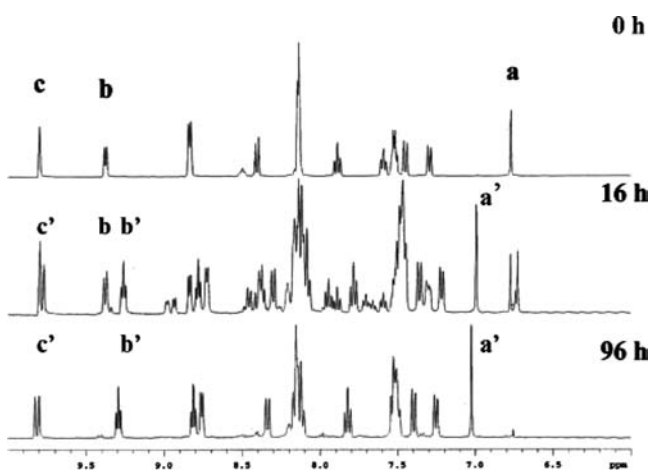


Figure 7. ^1H NMR spectra (6–10 ppm) of reaction mixture containing **3** (10 mM) and GSH (40 mM), after a time interval of 0 h (top), 16 h (middle), and 96 h (bottom) in D_2O .

change was observed. As the time progressed over the course of 96 h,⁸⁴ original resonances diminished and new resonances appeared. Major changes were noted with resonances at 6.6, 9.4, and 9.9 ppm (Figure 7, labeled a–c, respectively). The resonance at 6.6 ppm (a), assigned to the methine proton of the ligand N4PyCO₂Me, shifted to 7.0 ppm (a') over time. A resonance assigned to the pyridyl protons of the ligand at 9.4 ppm (b) disappeared with concomitant growth of a new resonance at 9.2 ppm (b'). The resonance at 9.8 ppm (c) split to form two peaks (c') with similar intensities. On the basis of the distance between the peaks (9.7 Hz), which are too large for ^1H – ^1H coupling in a pyridine ring, and the lack of cross peaks in 2D-COSY correlation spectrum (SI), the two peaks are assigned as independent singlets rather than a doublet. This is consistent with the formation of a 1:1 mixture of diastereomers of **5**, which occurs because both starting

materials are chiral, where **3** is racemic and GSH is enantioenriched. Also, shifts in the peaks corresponding to cys_α (4.5 \rightarrow 4.3 ppm) and cys_β (2.9 \rightarrow 3.1 ppm) protons of GSH (SI) were observed, consistent with the direct thiolate ligation to the cobalt center.^{36,56} All resonances lie within the 1–10 ppm region, confirming that **5** is a low-spin Co(III) complex. Furthermore, even after 96 h, resonances were still sharp and well-defined, and no broadening occurred. This is consistent with a lack of paramagnetic impurities, as would be expected if diamagnetic **3** or **5** was reduced by GSH to form a Co(II) complex during the reaction. Less than 5% of the total GSH was oxidized to form GSSG, as judged by ^1H NMR spectroscopy, which confirmed a negligible role for oxidation of GSH by atmospheric O_2 in this process, either uncatalyzed or catalyzed by **3**. Taken together, these data confirm that the reaction of **3** with GSH proceeds cleanly to generate **5** under these conditions.

The high-resolution ESMS spectrum of **5** generated *in situ* displayed a prominent ion cluster with a peak at $m/z = 395.5974$. This cluster displayed an isotopic pattern that fits with molecular formula $[\text{Co}(\text{N4PyCO}_2\text{Me})(\text{SG})]^{2+}$ (Figure 8),

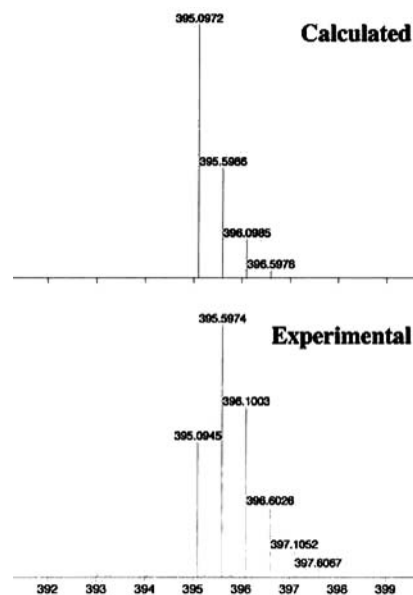


Figure 8. Calculated (top) and observed (bottom) high resolution mass spectra (HRMS) for the dication $[\text{Co}^{\text{III}}(\text{N4PyCO}_2\text{Me})(\text{SG})]^{2+}$ of **5**. See text for more details.

although the intensities of calculated and experimental isotopic pattern do not correlate exactly. In this dication, the ligand derived from GSH is treated as a monoanion (i.e., GSH-H^+), as would be expected if the thiolate of GSH were deprotonated and bound to the Co(III) center of **5**. The difference in intensities from the calculated spectrum may indicate that **5** is partially reduced to form $[\text{Co}(\text{II})(\text{N4PyCO}_2\text{Me})(\text{GSH})]^{2+}$ under the harsh conditions of analysis (150 $^\circ\text{C}$, 40 V).

Like compound **3**, the Co(III) complex $[\text{Co}(\text{Bn-CDPy3})\text{-Cl}]\text{Cl}_2$ (**4**) reacts with GSH in 100 mM acetate buffer to generate the species $[\text{Co}(\text{Bn-CDPy3})(\text{SG})]^{2+}$ (**6**). The reaction of **4** (0.5 mM) with GSH (10 mM) was followed by UV-vis spectroscopy over time at $298 \pm 2 \text{ K}$ (Figure 9a). As with **3**, the disappearance of a peak at 555 nm and appearance of two new peaks at 320 and 580 nm were observed, with shoulders at 500 and 450 nm. In addition, two isosbestic points

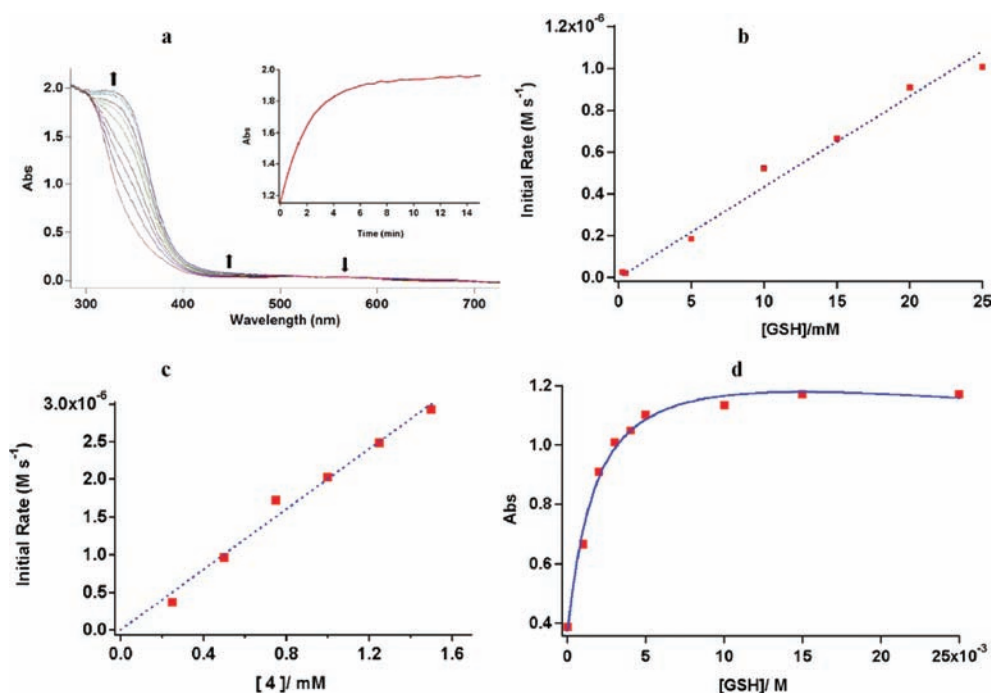


Figure 9. (a) UV-vis spectral change for **4** (0.5 mM) upon reaction with GSH (10 mM) in 100 mM acetate buffer at 298 ± 2 K (inset: Abs vs time plot for growth of peak at 320 nm). (b) Plot of the initial rate of reaction vs [GSH] for substitution of Cl^- with GSH (0.5–25.0 mM) in **4** (0.5 mM) in 100 mM acetate buffer. (c) Plot of the initial rate of reaction vs [4] for substitution of Cl^- with GSH (25 mM) in **4** (0.25–1.5 mM) in 100 mM acetate buffer. (d) Abs_{320} vs [GSH] plot, obtained from the equilibrated solutions of **4** (0.5 mM) and GSH (0.0–25.0 mM) kept at 298 ± 2 K for 3 h (the data was fit according to the literature method, fixing $[\text{4}] = 5.0 \times 10^{-4}$ M, $A_{320}(\text{4}) = 0.378$ and $A_{320}(\text{6}) = 1.170$).³⁷

were present at 520 and 610 nm. The new peak at 320 nm is consistent with a $\text{S} \rightarrow \text{Co(III)}$ LMCT band, and with the thiolate of GSH binding to the Co(III) center of **6**. Kinetic and thermodynamic analysis indicated that the observed rates and equilibrium constant for formation of **6** were similar to **5**. The reaction of **4** with GSH follows the rate law, $\text{rate} = k_2[\text{4}][\text{GSH}]$ under the condition used in this study, the same as with **3**. The order of the reaction is unity with respect to both **4** and GSH as evidenced from the straight lines obtained when the initial rates of the reaction of **4** (0.5 mM) with GSH (0.5–25 mM) were plotted against the total concentration of GSH (Figure 9b), and when the initial rates of the reaction of GSH (25 mM) with **4** (0.25–1.5 mM) were plotted against the concentration of **4** (Figure 9c). The second-order rate constant, k_2 , of $8.7 \times 10^{-2} \text{ M}^{-1} \text{ s}^{-1}$ and $8.0 \times 10^{-2} \text{ M}^{-1} \text{ s}^{-1}$ were obtained from the individual plots which are in good agreement within the experimental error. A value of $740 \pm 47 \text{ M}^{-1}$ was obtained for the observed equilibrium constant, K_{obs} , for formation of **6** compared to $870 \pm 50 \text{ M}^{-1}$ for **5** in 100 mM acetate buffer (Figure 9d).

The species $[\text{Co}(\text{Bn-CDPy3})(\text{SG})]^{2+}$ (**6**), obtained from reaction of **4** and GSH *in situ*, was characterized further by UV-vis and ^1H NMR spectroscopies and mass spectrometry. Like **3**, new resonance peaks were observed when **4** (10 mM) was treated with GSH (40 mM) in D_2O , though the complete conversion of **4** into **6** was not observed. However, evolution of a new ion cluster with a dominant peak at $m/z = 421.1452$ was observed by ESMS, which agrees well with that expected for a dication with the chemical formula $[\text{Co}(\text{Bn-CDPy3})(\text{SG})]^{2+}$ of **6** (Figure 10). The time scale for evolution of this new peak correlated well with the time scale of the new peak at 320 nm from the kinetic experiments, consistent with its assignment as **6**. Using the maximum absorbance observed for reaction of **4**

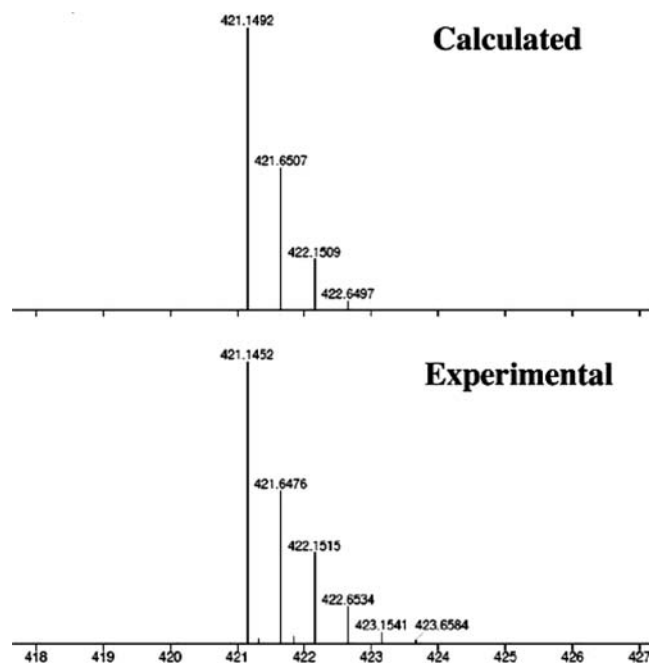


Figure 10. Calculated (top) and observed (bottom) high resolution mass spectra (HRMS) for the dication $[\text{Co}(\text{Bn-CDPy3})(\text{SG})]^{2+}$ of **6**.

(0.5 mM) with GSH (10 mM), a molar extinction coefficient of $\epsilon_{320} = 4300 \text{ M}^{-1} \text{ cm}^{-1}$ was calculated for **6**, which agrees with the intensity and wavelength of $\text{S} \rightarrow \text{Co(III)}$ LMCT bands observed for **5** and other related complexes.^{47,66,82} Taken together, these data are consistent with **4**, which contains an N5 donor set like that of H_2OCbl^+ and **3**, undergoing glutathionylation. Thus, glutathionylation appears to be a

general reaction of N5 donor Co(III) complexes that contain a labile coordination site, although reaction mechanisms and rates of glutathionylation differ between related complexes.

DISCUSSION

Glutathionylation of Cbl to form GSCbl is an important reaction in biology. Although this process is well understood at the fundamental chemistry level,^{31,37,85} the role of GSCbl in Cbl metabolism and its applications in medicine are still being actively investigated. Studies reported herein are significant, because they are the first example of synthetic Co(III) model compounds bearing a unique polypyridyl ligand set mimicking the chemistry of Cbl and undergoing glutathionylation in a similar fashion to H₂OCbl⁺. Data for **5** and **6**, which were generated *in situ* and characterized in solution by ¹H NMR (only **5**) and UV-vis spectroscopies and mass spectrometry, are consistent with ligation of the cysteine thiolate of GSH to the Co(III) centers, as occurs in GSCbl. Despite the fact that **5**, **6**, and GSCbl have similar structures, containing N5S donor atom sets and low-spin Co(III) centers, the formation of **5** and **6** occurs much more slowly (~100 times) than GSCbl at pH 5.0. The reaction of **3** or **4** with GSH was found to be bimolecular in nature, the order of reaction being unity with respect to each reactant. The pH dependence studies (pH 4.0–8.0) further confirmed that the rates for the substitution reaction increase with increasing pH, as would be expected, because of the higher concentration of GS⁻. This is different from H₂OCbl⁺, where the observed rate constants for the reaction of GSH with H₂OCbl⁺ were found to decrease with increasing pH, presumably because of increase in concentration of hydroxycobalamin (HOCbl), which does not react with GSH and hence decreases the rate of reaction.³⁷ This same issue does not apply to **3** and **4**, which have chloride rather than H₂O bound at the sixth position. Discrepancies regarding the mechanism of the axial ligand substitution reactions of vitamin B₁₂, its derivatives, and model complexes have been seen in the literature. The associative mechanism has been favored by some authors⁸⁶ whereas a limiting dissociative (D) mechanism^{87–91} or a dissociative interchange (I_d) mechanism^{63,92–100} has been favored by others. High-pressure kinetic techniques^{101–103} can differentiate between D or I_d substitution mechanism.^{63,94–96,101–104} Further studies will be required to elucidate the exact mechanism of substitution of Cl⁻ in **3** and **4** by GSH. Nonetheless, the kinetics of glutathionylation are clearly second-order.

In contrast to **3** and **4**, corrin and porphyrin-derived Co(III) complexes react much faster in ligand substitution reactions, where data suggests a dissociative interchange mechanism takes place.^{92,93,97} Difference in kinetics may be due to the nature of the ligand structure. In the delocalized structure of H₂OCbl⁺, the Co(III) oxidation state may be a formalism, where the complex is more like Co(II) due to delocalization into the corrin ring.^{105–107} This idea was recently supported with Cbl derivatives. A significant decrease in the rate of ligand substitution was observed with the stable yellow aquacyanocobyrinic acid heptamethyl ester, which contains less conjugation in the corrin ligand than H₂OCbl⁺.¹⁰⁸ Even though the kinetics and reaction pathways for glutathionylation of H₂OCbl⁺ differ from that of complexes **3** and **4**, it is significant that these synthetic model compounds mimic the chemistry of H₂OCbl⁺, which implies that Co(III) complexes related to Cbl used in biological studies may become glutathionylated in cell culture

and *in vivo*, especially with complexes containing labile ligands such as chloride or H₂O.

Glutathionylation of H₂OCbl⁺ occurs readily, and GSCbl is one of the most abundant forms of Cbl isolated from mammalian cells. Previous studies reported rate constants as high as 163 ± 8 M⁻¹ s⁻¹ (4.5 < pH < 11.0) for the formation of GSCbl.³⁷ Unlike H₂OCbl⁺, compounds **3** and **4** react slower with GSH, with rate constants ranging from 8.3 to 9.3 M⁻¹ s⁻¹, respectively. The slower rates of formation for **5** and **6** may be attributed to differences in ligand structure. Unlike corrin rings or planar oxime/Schiff base ligands found in cobalamin or cobaloxime, which contain large planar conjugated rings, the polypyridyl rings in **3** and **4** cannot adopt the same conformation, which may limit the amount of delocalization.

The observed equilibrium constants, K_{obs}, for the formation of **5** and **6** ranged between 740 and 870 M⁻¹, which are considerably smaller than earlier reported values of K_{obs} for GSCbl formation, of (9.5 ± 0.9) × 10⁶ M⁻¹ (pH 5.0, 25 °C),³⁷ (~5) × 10⁵ M⁻¹ (pH 4.7, temperature not specified),⁸⁵ and (1.1 ± 0.3) × 10⁵ M⁻¹ (pH 5.0, 25 °C)³¹ and also K_{obs} for [Me(Co)(tn)SG] formation where tn = 2,3,9,10-tetramethyl-1,4,8,11-tetra-azaundeca-1,3,8,10-tetraen-11-ol-1-olato anion, of ~10^{6.6} M⁻¹ (pH 7.0, temperature not specified).⁶⁶ The high formation constants of thiolate-bound vitamin B₁₂ model complexes have been attributed to π-bonding from the ligand to the cobalt center.⁴⁷ The lower values of K_{obs} for **5** and **6** may be attributed to weak interactions of thiolate ligands with Co(III) center, as a result of steric hindrance of GSH with N4PyCO₂Me and Bn-CDPy3 ligands on the cobalt center. Alternatively, backbonding could be lower because of electronic considerations. The lower value of K_{obs} for **6** as compared to **5** can also be explained because of the fact that the Co center is crowded in **6** as compared to **5** (based on crystallographic data), resulting in a weaker bonding interaction between the thiolate and Co(III) center. By changing the electronic structure of the ligand around the Co(III) center, the kinetic and equilibrium parameters for glutathionylation may be tuned.

CONCLUSION

Glutathionylation of synthetic Co(III) model compounds **3** and **4** was reported that mimics the biological chemistry of Cbl. These compounds show similar chemistry to H₂OCbl⁺, although kinetic and thermodynamic parameters differ. Unlike H₂OCbl⁺, where the Co(III) center is bound by the highly delocalized corrin ring and GSCbl formation is rapid and highly favorable, compounds **3** and **4** react slower with GSH in substitution reactions, and formation constants are not as strong. These results entail the importance of ligand structure toward tuning the special reactivity of H₂OCbl⁺. Nonetheless, the ease with which complexes such as **3** and **4** undergo Glutathionylation suggests this may be a general reaction for cobalt complexes of this type. Understanding how facile Glutathionylation is for synthetic cobalt complexes may lead to a better understanding of the behavior of these interesting metal complexes in biological systems, due to the natural abundance of GSH.

ASSOCIATED CONTENT

Supporting Information

Additional figures and tables. This material is available free of charge via the Internet at <http://pubs.acs.org>.

■ AUTHOR INFORMATION

Corresponding Author

*E-mail: jkodanko@chem.wayne.edu.

Notes

The authors declare no competing financial interest.

■ ACKNOWLEDGMENTS

We would like to acknowledge Wayne State University for its generous support of this research. J.P. acknowledges the Thomas C. Rumble Fellowship. We thank Mary Jane Heeg for X-ray crystallographic analysis of 3.

■ REFERENCES

- (1) Weir, D. G.; Scott, J. M. *Baillieres Clin. Haematol.* **1995**, *8*, 479–497.
- (2) Chanarin, I. *Br. J. Haematol.* **2000**, *111*, 407–415.
- (3) McCaddon, A.; Regland, B.; Hudson, P.; Davies, G. *Neurology* **2002**, *58*, 1395–1399.
- (4) Collin, S. M.; Metcalfe, C.; Refsum, H.; Lewis, S. J.; Zuccolo, L.; Smith, G. D.; Chen, L.; Harris, R.; Davis, M.; Marsden, G.; Johnston, C.; Lane, J. A.; Ebbing, M.; Bona, K. H.; Nygard, O.; Ueland, P. M.; Grau, M. V.; Baron, J. A.; Donovan, J. L.; Neal, D. E.; Hamdy, F. C.; Smith, A. D.; Martin, R. M. *Cancer Epidemiol., Biomarkers Prev.* **2010**, *19*, 1632–1642.
- (5) Weissbach, H.; Taylor, R. T. *Fed. Proc.* **1966**, *25*, 1649–1656.
- (6) Taylor, R. T.; Hanna, M. L. *Arch. Biochem. Biophys.* **1975**, *171*, 507–520.
- (7) Gurnani, S.; Mistry, S. P.; Johnson, B. C. *Biochim. Biophys. Acta* **1960**, *38*, 187–188.
- (8) Cannata, J. J. B.; Focesi, A. Jr.; Mazumder, R.; Warner, R. C.; Ochoa, S. J. *Biol. Chem.* **1965**, *240*, 3249–3252.
- (9) Kelly, P. J.; Rosand, J.; Kistler, J. P.; Shih, V. E.; Silveira, S.; Plomaritoglou, A.; Furie, K. L. *Neurology* **2002**, *59*, 529–536.
- (10) Kawamoto, R.; Kajiwara, T.; Oka, Y.; Takagi, Y. *J. Atheroscler. Thromb.* **2002**, *9*, 121–125.
- (11) Ogawa, M.; Abe, S.; Saigo, M.; Biro, S.; Toda, H.; Matsuoka, T.; Torii, H.; Minagoe, S.; Maruyama, I.; Tei, C. *Thromb. Res.* **2003**, *109*, 253–258.
- (12) Biswas, S.; Chida, A. S.; Rahman, I. *Biochem. Pharmacol.* **2006**, *71*, 551–564.
- (13) Ginnan, R.; Guikema, B. J.; Halligan, K. E.; Singer, H. A.; Jourd'heuil, D. *Free Radical Biol. Med.* **2008**, *44*, 1232–1245.
- (14) McCaddon, A.; Davies, G.; Hudson, P.; Tandy, S.; Cattell, H. *Int. J. Geriatr. Psych.* **1998**, *13*, 235–239.
- (15) Nilsson, K.; Gustafson, L.; Hultberg, B. *Dementia Geriatr. Cognit. Disord.* **2002**, *14*, 7–12.
- (16) Vafai, S. B.; Stock, J. B. *FEBS Lett.* **2002**, *518*, 1–4.
- (17) Seshadri, S.; Beiser, A.; Selhub, J.; Jacques, P. F.; Rosenberg, I. H.; D'Agostino, R. B.; Wilson, P. W. F.; Wolf, P. A. *N. Engl. J. Med.* **2002**, *346*, 476–483.
- (18) Hodgkin, D. C.; Kamper, J.; Mackay, M.; Pickworth, J.; Trueblood, K. N.; White, J. G. *Nature* **1956**, *178*, 64–66.
- (19) Seetharam, B.; Bose, S.; Li, N. J. *Nutr.* **1999**, *129*, 1761–1764.
- (20) Quadros, E. V.; Regec, A. L.; Khan, K. M. F.; Quadros, E.; Rothenberg, S. P. *Am. J. Physiol.* **1999**, *277*, G161–G166.
- (21) Quadros, E. V.; Nakayama, Y.; Sequeira, J. M. *Biochem. Biophys. Res. Commun.* **2005**, *327*, 1006–1010.
- (22) Zhao, R.; Lind, J.; Merenyi, G.; Eriksen, T. E. *J. Chem. Soc., Perkin Trans. 2* **1997**, 569–574.
- (23) Griffith, O. W. *Free Radical Biol. Med.* **1999**, *27*, 922–935.
- (24) Hannibal, L.; Axhemi, A.; Glushchenko, A. V.; Moreira, E. S.; Brasch, N. E.; Jacobsen, D. W. *Clin. Chem. Lab. Med.* **2008**, *46*, 1739–1746.
- (25) Birch, C. S.; Brasch, N. E.; McCaddon, A.; Williams, J. H. H. *Free Radical Biol. Med.* **2009**, *47*, 184–188.
- (26) Pezacka, E.; Green, R.; Jacobsen, D. W. *Biochem. Biophys. Res. Commun.* **1990**, *169*, 443–450.
- (27) McCaddon, A.; Hudson, P. R. *Future Neurol.* **2007**, *2*, 537–547.
- (28) Suto, R. K.; Brasch, N. E.; Anderson, O. P.; Finke, R. G. *Inorg. Chem.* **2001**, *40*, 2686–2692.
- (29) Scheuring, E. M.; Sagi, I.; Chance, M. R. *Biochemistry* **1994**, *33*, 6310–6315.
- (30) Conrad, K. S.; Brunold, T. C. *Inorg. Chem.* **2011**, *50*, 8755–8766.
- (31) Brasch, N. E.; Hsu, T.-L. C.; Doll, K. M.; Finke, R. G. *J. Inorg. Biochem.* **1999**, *76*, 197–209.
- (32) Schumacher, L. A.; Mukherjee, R.; Brown, J. M.; Subedi, H.; Brasch, N. E. *Eur. J. Inorg. Chem.* **2011**, 4717–4720.
- (33) Li, S.-x.; Deng, N.-s.; Zheng, F.-y. *Bioorg. Med. Chem. Lett.* **2004**, *14*, 505–510.
- (34) Brasch, N. E.; Xia, L. Method of Synthesis of β -Thiolato Cobalamin Nucleoside Compounds. U.S. Patent 7,030,105 B2, April 18, 2006.
- (35) Wagner, F.; Bernhauer, K. *Ann. N.Y. Acad. Sci.* **1964**, *112*, 580–589.
- (36) Brown, K. L.; Zou, X.; Savon, S. R.; Jacobsen, D. W. *Biochemistry* **1993**, *32*, 8421–8428.
- (37) Xia, L.; Cregan, A. G.; Berben, L. A.; Brasch, N. E. *Inorg. Chem.* **2004**, *43*, 6848–6857.
- (38) Shevell, M. L.; Rosenblatt, D. S. *Can. J. Neurol. Sci.* **1992**, *19*, 472–486.
- (39) Zheng, D.; Birke, R. L. *J. Am. Chem. Soc.* **2002**, *124*, 9066–9067.
- (40) Randaccio, L.; Geremia, S.; Nardin, G.; Slouf, M.; Srnova, I. *Inorg. Chem.* **1999**, *38*, 4087–4092.
- (41) Randaccio, L.; Furlan, M.; Geremia, S.; Slouf, M.; Srnova, I.; Toffoli, D. *Inorg. Chem.* **2000**, *39*, 3403–3413.
- (42) Randaccio, L.; Geremia, S.; Stener, M.; Toffoli, D.; Zangrando, E. *Eur. J. Inorg. Chem.* **2002**, 93–103.
- (43) Hannibal, L.; Smith, C. A.; Jacobsen, D. W. *Inorg. Chem.* **2010**, *49*, 9921–9927.
- (44) Conrad, K. S.; Brunold, T. C. *Inorg. Chem.* **2011**, *50*, 8755–8766.
- (45) Crumbliss, A. L.; Wilmarth, W. K. *J. Am. Chem. Soc.* **1970**, *92*, 2593–2594.
- (46) Brown, K. L.; Satyanarayana, S. *J. Am. Chem. Soc.* **1992**, *114*, 5674–5684.
- (47) Brown, K. L.; Kallen, R. G. *J. Am. Chem. Soc.* **1972**, *94*, 1894–1901.
- (48) Marzilli, L. G.; Toscano, P. J.; Randaccio, L.; Bresciani-Pahor, N.; Calligaris, M. *J. Am. Chem. Soc.* **1979**, *101*, 6754–6756.
- (49) Randaccio, L.; Bresciani-Pahor, N.; Toscano, P. J.; Marzilli, L. G. *J. Am. Chem. Soc.* **1980**, *102*, 7372–7373.
- (50) Bresciani-Pahor, N.; Randaccio, L.; Toscano, P. G.; Sandercock, A. C.; Marzilli, L. G. *J. Chem. Soc., Dalton Trans.* **1982**, 129–134.
- (51) Summers, M. F.; Toscano, P. J.; Bresciani-Pahor, N.; Nardin, G.; Randaccio, L.; Marzilli, L. G. *J. Am. Chem. Soc.* **1983**, *105*, 6259–6263.
- (52) Bresciani-Pahor, N.; Marzilli, L. G.; Randaccio, L.; Toscano, P. J.; Zangrando, E. *J. Chem. Soc., Chem. Commun.* **1984**, 1508–1510.
- (53) Bresciani-Pahor, N.; Forcolin, M.; Marzilli, L. G.; Randaccio, L.; Summers, M. F.; Toscano, P. J. *Coord. Chem. Rev.* **1985**, *63*, 1–125.
- (54) Marzilli, L. G.; Summers, M. F.; Zangrando, E.; Bresciani-Pahor, N.; Randaccio, L. *J. Am. Chem. Soc.* **1986**, *108*, 4830–4838.
- (55) Randaccio, L.; Pahor, N. B.; Zangrando, E.; Marzilli, L. G. *Chem. Soc. Rev.* **1989**, *18*, 225–250.
- (56) Polson, S. M.; Hansen, L.; Marzilli, L. G. *Inorg. Chem.* **1997**, *36*, 307–313.
- (57) Costa, G.; Mestroni, G.; De Savognani, E. *Inorg. Chim. Acta* **1969**, *3*, 323–328.
- (58) Costa, G.; Puxeddu, A.; Reisenhofer, E. *Collect. Czech. Chem. Commun.* **1971**, *36*, 1065–78.
- (59) Costa, G. *Coord. Chem. Rev.* **1972**, *8*, 63–75.
- (60) Costa, G.; Mestroni, G.; Tauzher, G.; Stefani, L. *J. Organomet. Chem.* **1966**, *6*, 181–187.
- (61) Costa, G.; Mestroni, G.; Stefani, L. *J. Organomet. Chem.* **1967**, *7*, 493–501.

- (62) Bigotto, A.; Costa, G.; Mestroni, G.; Nardin-Stefani, L.; Puxeddu, A.; Reisenhofer, E.; Tauzher, G. *Inorg. Chim. Acta, Rev.* **1970**, *4*, 41–49.
- (63) Hamza, M. S. A.; Duecker-Benfer, C.; Van Eldik, R. *Inorg. Chem.* **2000**, *39*, 3777–3783.
- (64) Brown, K. L.; Chernoff, D.; Keljo, D. J.; Kallen, R. G. *J. Am. Chem. Soc.* **1972**, *94*, 6697–6704.
- (65) Brown, K. L.; Awtrey, A. W. *Inorg. Chem.* **1978**, *17*, 111–119.
- (66) Pellizer, G.; Tauszik, G. R.; Costa, G. *J. Chem. Soc., Dalton Trans.* **1973**, 317–322.
- (67) Roelfes, G.; Branum, M. E.; Wang, L.; Que, L. Jr.; Feringa, B. L. *J. Am. Chem. Soc.* **2000**, *122*, 11517–11518.
- (68) Hammoud, M. M.; McKamie, J. J.; Heeg, M. J.; Kodanko, J. J. *Dalton Trans.* **2008**, 4843–4845.
- (69) Abouelatta, A. I.; Sonk, J. A.; Hammoud, M. M.; Zurcher, D. M.; McKamie, J. J.; Schlegel, H. B.; Kodanko, J. J. *Inorg. Chem.* **2010**, *49*, 5202–5211.
- (70) Elgy, C. N.; Wells, C. F. *J. Chem. Soc., Dalton Trans.* **1980**, 2405–2409.
- (71) Springborg, J.; Schaeffer, C. E. *Acta Chem. Scand.* **1973**, *27*, 3312–3322.
- (72) Sheldrick, G. M. *Acta Crystallogr., Sect. A* **2008**, *A64*, 112–122.
- (73) APEX-II collection and processing programs are distributed by the manufacturer: Bruker AXS Inc., Madison, Wisconsin, 2005.
- (74) Jackson, W. G.; Dickie, A. J.; Bhula, R.; McKeon, J. A.; Spiccia, L.; Brudenell, S. J.; Hockless, D. C. R.; Willis, A. C. *Inorg. Chem.* **2004**, *43*, 6549–6556.
- (75) Poth, T.; Paulus, H.; Elias, H.; Van Eldik, R.; Grohmann, A. *Eur. J. Inorg. Chem.* **1999**, 643–650.
- (76) The mean value for Co(III)–N bond lengths in classical complexes, both aliphatic and py, is 1.96(1) Å using survey parameters $(\text{NH}_3)_6\text{Co(III)}^{3+}$, $(\text{en})_3\text{Co(III)}^{3+}$, and NSCo(III)Cl^{2+} . The mean Co–Cl distance in the latter category is 2.26(2) Å. *Cambridge Structural Database*; Cambridge, U.K., 2009.
- (77) Bombieri, G.; Forsellini, E.; Del Pra, A.; Tobe, M. L. *Inorg. Chim. Acta* **1981**, *51*, 177–183.
- (78) McLachlan, G. A.; Brudenell, S. J.; Fallon, G. D.; Martin, R. L.; Spiccia, L.; Tiekink, E. R. T. *J. Chem. Soc., Dalton Trans.* **1995**, 439–447.
- (79) Kojima, T.; Weber, D. M.; Choma, C. T. *Acta Crystallogr., Sect. E* **2005**, *E61*, m226–m228.
- (80) Geary, W. J. *Coord. Chem. Rev.* **1971**, *7*, 81–122.
- (81) Rabenstein, D. L. *J. Am. Chem. Soc.* **1973**, *95*, 2797–2803.
- (82) Higgs, T. C.; Ji, D.; Czernuszewicz, R. S.; Matzanke, B. F.; Schunemann, V.; Trautwein, A. X.; Helliwell, M.; Ramirez, W.; Carrano, C. J. *Inorg. Chem.* **1998**, *37*, 2383–2392.
- (83) Gahan, L. R.; Hughes, J. G.; O'Connor, M. J.; Oliver, P. J. *Inorg. Chem.* **1979**, *18*, 933–937.
- (84) This reaction is slower because only a 4-fold excess of GSH is used and pD of reaction mixture was ~3.0 in D₂O
- (85) Adler, N.; Medwick, T.; Poznanski, T. J. *J. Am. Chem. Soc.* **1966**, *88*, 5018–5020.
- (86) Brasch, N. E.; Hamza, M. S. A.; Van Eldik, R. *Inorg. Chem.* **1997**, *36*, 3216–3222.
- (87) Thusius, D. *J. Am. Chem. Soc.* **1971**, *93*, 2629–2635.
- (88) Nome, F.; Fendler, J. H. *J. Chem. Soc., Dalton Trans.* **1976**, 1212–1219.
- (89) Baldwin, D. A.; Betterton, E. A.; Pratt, J. M. S. *Afr. J. Chem.* **1982**, *35*, 173–175.
- (90) Stochel, G.; Van Eldik, R.; Kunkely, H.; Vogler, A. *Inorg. Chem.* **1989**, *28*, 4314–4318.
- (91) Stochel, G.; Van Eldik, R. *Inorg. Chem.* **1990**, *29*, 2075–2077.
- (92) Randall, W. C.; Alberty, R. A. *Biochemistry* **1967**, *6*, 1520–1525.
- (93) Reenstra, W. W.; Jencks, W. P. *J. Am. Chem. Soc.* **1979**, *101*, 5780–5791.
- (94) Prinsloo, F. F.; Meier, M.; van Eldik, R. *Inorg. Chem.* **1994**, *33*, 900–904.
- (95) Meier, M.; van Eldik, R. *Inorg. Chem.* **1993**, *32*, 2635–2639.
- (96) Prinsloo, F. F.; Breet, E. L. J.; van Eldik, R. *J. Chem. Soc., Dalton Trans.* **1995**, 685–688.
- (97) Marques, H. M. *J. Chem. Soc., Dalton Trans.* **1991**, 339–341.
- (98) Marques, H. M.; Bradley, J. C.; Campbell, L. A. *J. Chem. Soc., Dalton Trans.* **1992**, 2019–2027.
- (99) Marques, H. M.; Bradley, J. C.; Brown, K. L.; Brooks, H. J. *J. Chem. Soc., Dalton Trans.* **1993**, 3475–3478.
- (100) Marques, H. M.; Munro, O. Q.; Cumming, B. M.; de Nysschen, C. *J. Chem. Soc., Dalton Trans.* **1994**, 297–303.
- (101) *Inorganic High Pressure Chemistry: Kinetics and Mechanisms*; Van Eldik, R., Ed.; Studies in Inorganic Chemistry; 1986; Vol. 7, p 448.
- (102) Van Eldik, R.; Asano, T.; Le Noble, W. J. *Chem. Rev.* **1989**, *89*, 549–688.
- (103) Drljaca, A.; Hubbard, C. D.; Van Eldik, R.; Asano, T.; Basilevsky, M. V.; Le Noble, W. J. *Chem. Rev.* **1998**, *98*, 2167–2289.
- (104) Leipoldt, J. G.; Van Eldik, R.; Kelm, H. *Inorg. Chem.* **1983**, *22*, 4146–4149.
- (105) Perry, C. B.; Fernandes, M. A.; Brown, K. L.; Zou, X.; Valente, E. J.; Marques, H. M. *Eur. J. Inorg. Chem.* **2003**, 2095–2107.
- (106) Knapton, L.; Marques, H. M. *Dalton Trans.* **2005**, 889–895.
- (107) Brown, K. L.; Cheng, S.; Zou, X.; Zubkowski, J. D.; Valente, E. J.; Knapton, L.; Marques, H. M. *Inorg. Chem.* **1997**, *36*, 3666–3675.
- (108) Chemaly, S. M.; Florczak, M.; Dirr, H.; Marques, H. M. *Inorg. Chem.* **2011**, *50*, 8719–8727.